Check for updates

Neurotrauma Reports
Volume 7.1, 2026
DOI: 10.1177/2689288X251411057

Neurotrauma Reports
Mary Ann Liebert
A Part of Sage

REGULAR ARTICLE Open Access

Genetic Diversity Influences Response and Outcome to Blast Traumatic Brain Injury in a Murine Model

Anastasia P. Georges,[1] Kevin D. Browne,[2,3] Daunel V. Augustin,[1] Adedotun H. Bello,[2,3] D. Kacy Cullen,[1–3] and David F. Meaney[1,2,*]

Abstract

Blast-induced traumatic brain injury (bTBI) is a significant health concern for military personnel, causing potential long-term neurological consequences. Given the unique and heterogeneous genetic makeup of the human population, the acute responses and evolving sequelae from blast exposure are difficult to predict. To address these challenges, murine models are invaluable in the study of bTBI, as they allow researchers to carefully control exposure parameters while examining physiological changes across genetic, cellular, and whole-organism levels over time. In this study, we investigated the role of genetic diversity in bTBI by examining six common mouse strains—A/J, 129S1/SvImJ, NOD/ShiLtJ, NZO/HlLtJ, C57BL/6J, and CAST/EiJ—and their possible differential response to blast overpressure. We assessed immediate neurological impairment, respiratory symptoms, lethality thresholds, and gross pathological and histological changes following blast overpressure exposure across these strains. We observed significant strain-dependent differences across all the measured outcomes. In particular, C57BL/6J mice exhibited the longest normalized righting times and highest incidence of subdural hematomas. Notably, the strains used as models of type I/II diabetes (NZO/HlLtJ and NOD/ShiLtJ) showed the highest resilience to blast-induced lethality. In comparison, the CAST/EiJ strain was the most susceptible to immediate apnea and had the lowest lethality threshold. The NZO/HlLtJ mice showed the highest incidence of pulmonary bleeding. Our findings highlight the substantial influence of the genetic background on the bTBI outcomes in mice, even with highly controlled physical exposure conditions. This comprehensive characterization of strain-dependent responses to bTBI provides a foundation for investigating the genetic influences on blast injury outcomes and developing more targeted preventative and/or therapeutic strategies for bTBI.

Keywords: blast traumatic brain injury; collaborative cross; founder strains; genetic diversity

Introduction

Traumatic brain injury (TBI), particularly blast-induced TBI (bTBI), has emerged as a significant health concern for military personnel. The prevalence of TBI among U.S. service members deployed to recent conflict zones has been estimated at 15–23%, with blast exposure being a primary cause.[1] These injuries can lead to long-term neurological deficits, cognitive impairment, and

[1]Department of Bioengineering, School of Engineering and Applied Science, Philadelphia, Pennsylvania, USA.
[2]Department of Neurosurgery, Center for Brain Injury and Repair, Perelman School of Medicine, Philadelphia, Pennsylvania, USA.
[3]Center for Neurotrauma, Neurodegeneration and Restoration, Corporal Michael J. Crescenz VA Medical Center, Philadelphia, Pennsylvania, USA.
Any opinion, findings, and conclusions or recommendations expressed in this material are those of the author(s) and do not necessarily reflect the views of the Department of Veterans Affairs or the United States Government.

*Address correspondence to: David F. Meaney, PhD, Department of Bioengineering, School of Engineering and Applied Science, 3320 Smith Walk, Philadelphia, PA 19104-6392, USA; E-mail: dmeaney@seas.upenn.edu

© The Author(s) 2025. Published by Mary Ann Liebert (NY), LLC. This article is distributed under the terms of the Creative Commons Attribution-NonCommercial 4.0 License (https://creativecommons.org/licenses/by-nc/4.0/) which permits non-commercial use, reproduction and distribution of the work without further permission provided the original work is attributed as specified on the SAGE and Open Access page (https://us.sagepub.com/en-us/nam/open-access-at-sage).

psychological disorders, significantly impacting the affected individuals' operational readiness and quality of life. TBI is a heterogeneous condition with many different presentations and outcomes in patients, suggesting that factors beyond the primary injury mechanism(s) or severity affect recovery.[2] For instance, the genetic diversity in the human population may play a significant role in individual responses to TBI, including variations in susceptibility, severity of symptoms, and recovery outcomes. Clinical evidence supports the role of genetic factors in blast-related outcomes. Taylor et al. demonstrate that blast exposure interacts with the *5HTTLPR* genetic variant to predict posttraumatic stress symptoms independently of the TBI diagnosis.[84] These clinical findings highlight the critical need for preclinical models that incorporate genetic diversity to better recapitulate the heterogeneity observed in human blast injury outcomes.[3]

Preclinical models of bTBI are useful due to their homogeneity, control of experimental variables, and reproducibility, and there is no doubt that there is an emergent need for high-quality preclinical models.[4–7] However, the integration of genetic diversity enables the more robust identification of genetic risk factors, gene–environment interactions, and pharmacogenomic effects, which will potentially improve the translational value of preclinical studies. The majority of research uses C57BL/6 mice, which show behavioral and histopathological changes in response to blast exposure. While the importance of genetic predisposition to disease and injury has been stated, most work focuses on how alterations in a specific gene can affect the response to blast. For example, Tran et al. used *APOE3* and *APOE4* transgenic mouse models to investigate the role of the *APOE* genotype in blast-induced TBI outcomes, demonstrating gene-specific differences in neuroinflammation and behavior.[7,8] Additionally, Alzheimer's disease-related transgenic mice were used to evaluate the amyloid burden and tau-influenced dysregulation of learning pathways following bTBI.[9–11] However, these targeted transgenic studies do not directly mimic broad, genomic-level diversity.

In 2004, eight genetic strains, known as *founder strains*, were used to develop an inbred mouse population known as the Collaborative Cross (CC).[12] The eight founder strains—A/J, 129S1/SvlmJ, NOD/LtJ, NZO/HILtJ, C57BL/6J, CAst/EiJ, PWK/PhJ, WSB/EiJ—encompass 90% of the genetic diversity of the commonly used laboratory mice and three wild-derived strains.[13] While each of the chosen strains does not represent a well-known human condition, the genome of each strain is fully sequenced, with 45 million segregated single-nucleotide polymorphisms (SNPs).[14,15] As a result of intercrossing the CC, two additional multiparental populations (MPPs) were derived—the F1 hybrids of the CC (CC-RIX) and the Diversity Outbred (DO) populations.[16,17] These populations provide an even broader spectrum of genetic variation that closely resembles human genetic diversity.[14,18]

Both the CC and DO murine populations represent the genetic diversity of a whole population and thus provide a method to link phenotypes to potential causal genetic factors. For example, crossing the founder strains led to the identification of gene loci associated with specific neurobehavioral phenotypes.[19]Likewise, collaborative crossing in disease models uncovered additional gene loci that either relate to disease risk, poor outcome, or other key attributes of disease progression.[15,20–23] However, none of these collaborative crossing designs have been used in preclinical TBI models, nor correlated with the responses and outcomes to injury. Rather, past work is limited to studying some specific pairings of strains—one study compared the widely used strains C57BL/6J and BALB/cByJ mice with the Jackson Diversity Outbred (J:DO) murine population in a bTBI study,[9] while a second study utilized NOD/LtJ mice to examine adenosine monophosphate (AMP)-activated protein kinase (AMPK) and lymphoid cells following TBI.[24] Murray et al. utilize all the eight founder strains and examined hippocampal gene expression changes following blast-induced TBI. The findings support the influence of the genetic background on transcriptional regulation in response to bTBI.[25] Thus, while past work has addressed targeted genetic questions, including initial transcriptomic profiling across the founder strains, the field lacks a comprehensive foundation for comparing the acute response to blast exposure based on genetic diversity and phenotype, which could be a critical first step toward identifying potential risk factors in blast exposure.

In the current study, we used six of the founder strains of the CC (Table 1) to systematically investigate the role of genetic diversity in lethal thresholds, acute neurological impairments, and gross neuropathological and pulmonary damage following blast overpressure exposure. The C57BL/6J strain serves as a widely used control strain in neuroscience research,

Table 1. Characterization of Strains

Strain	*General characteristics*	*Phenotypes*	*Research applications*	*Potential risk factors for bTBI*
A/J	Hearing loss, challenging to breed, deficit in macrophage function, abnormal leukopoiesis[25]	Spontaneous lung adenomas, vulnerable to carcinogen-induced tumors, resistant to atherosclerosis, obesity, diabetes, and insulin[25]	Cancer, carcinogen testing, immunology, respiratory illnesses[25]	Susceptibility to respiratory symptoms, pulmonary damage, macrophage dysfunction
129S1/SvlmJ	Multiple embryonic stem cell lines[25]	Spontaneous testicular teratomas, corpus callosum defects[25]	Neuropsychiatric and social behavioral models, long-term neurological outcomes following virus, subarachnoid hemorrhage	129 × C57 hybrid TBI,[26] the role of the corpus callosum in injury and recovery
NOD/ShiLtJ	Autoimmune type 1 diabetes, hearing impaired[25]	Hyperglycemia, insulitis, immune deficits, impaired wound healing[25]	1 TBI study,[27] immunotherapy, type 1 diabetes mellitus (T1DM) studies, Sjorgen's syndrome[28,29]	The intersection of T1DM and bTBI;[30–33] immune system and bTBI
NZO/HlLtJ	Obesity, type 2 diabetes, hypertension, poor breeding[25]	High birth weights, impaired glucose intolerance, anti-insulin receptor antibodies, tumors[25]	Type 2 diabetes mellitus (T2DM) obesity studies, tumor modeling, metabolic disorders,[34]	The intersection of T2DM and bTBI,[35] obesity and bTBI
C57BL/6J	Most widely used strain, first strain to have its genome sequenced, age-related hearing loss[25]	Normal[25]	Broad research applications, general-purpose strain, maximal induced-mutation expression[25,36]	As the well-characterized mouse strain across all research disciplines, serves as a baseline to which all other strains are compared[25,36]
CAST/EiJ	Wild-derived, Thailand[25]	Resistant to flavivirus infection, Dorsal root ganglia (DRG) axonal growth following central nervous system (CNS) injury[25,37]	Axonal injury and nerve regeneration[37,38]	Wild-derived strains include genetic variation that exists in wild populations; characteristics represent biological adaptations

Comparison of general, whole body, and central nervous system (CNS) phenotypes, behavioral considerations, and research applications across the six genetic strains.

providing a standard against which other strains can be compared.[25,36] The A/J strain, known for its susceptibility to lung diseases,[25,36] was included to investigate the potential interplay between pulmonary vulnerability and blast-induced brain injury.[39–41] The 129S1/SvlmJ strain offers a well-characterized genetic profile.[26,42] The NOD/ShiLtJ and NZO/HILtJ strains were chosen for their utility in studying diabetes,[30,34] as clinical studies have shown that diabetes is a risk factor for poor outcomes following TBI.[35] The wild-derived CAST/EiJ strain introduces genetic diversity that may more closely reflect the natural variations seen in human populations.[43] This strain is commonly used to study the long-term effects of viral illnesses, including influenza, West Nile virus, and COVID-19.[44–47] Furthermore, as these selected strains collectively represent laboratory mouse genetic diversity and wild-derived genotypes, the findings among these strains can be linked to specific gene loci and haplotypes, rather than generalized human conditions.

By embracing genetic diversity in our preclinical model, we aim to provide a more nuanced understanding of blast-induced injuries and their genetic underpinnings. This approach has the potential to inform the development of personalized prevention strategies and treatments for blast-exposed individuals in military settings. Moreover, by correlating our findings with known clinical risk factors, we strive to bridge the gap between animal studies and human applications, ultimately contributing to improved care for those affected by blast-induced TBI.

Methods

Animals

In this study, we enrolled 8–10-week-old (w/o) male mice of each genetic strain (A/J, 129S1/SvlmJ, NOD/ShiLtJ, NZO/HILtJ, C57BL/6J, CAST/EiJ) (The Jackson Laboratory, Bar Harbor, ME, USA). All experimental procedures were approved by the Institutional Animal Care and Use Committees (IACUCs) at both the CMC Veterans Affairs Medical Center and the University of Pennsylvania. We carefully adhered to the guidelines set forth in the Public Health Service (PHS) Policy on Humane Care and Use of Laboratory Animals to ensure animal welfare.

Blast tube configuration and pressure transducer measurements

We adapted the shock tube design from Gullotti et al.[48] and oriented the aluminum tube in a vertical position.[49]

To initiate a blast peak overpressure wave, we supplied helium to the load chamber, where it burst through single-use polyethylene terephthalate (PET) membrane(s) of a precalculated thickness (Fig. 1). Pressures measured at the tube exit were used to quantify the blast overpressure exposure, as peak overpressure is linearly correlated with the membrane thickness (Fig. 1).

In designing our study, we considered various options for investigating the effects of blast overpressure, such as blast tube orientation (vertical, horizontal, or angled), animal placement (inside or outside the blast tube), and distance from the tube exit.[6,48,50] We chose a vertical orientation and fixed animal position at the tube exit to minimize head motion acceleration.[48] We also used a sorbothane-lined aluminum encasing to reduce lung damage and severe organ-wide injury. Our priority was to maintain consistent experimental parameters to preserve the physical characteristics of the loading direction and waveform shape.[50,51]

We measured the peak overpressure using a pressure transducer (model 8530B-200; Endevco, Irvine, CA, USA) positioned at the exit of the blast tube. To reduce noise in the signal, we used an inline filter conditioning device (linear phase filter, 10 kHz cutoff frequency; Alligator Technologies, Charlottesville, VA, USA). At least two test trials were used to calibrate the blast overpressure level caused by rupturing PET membranes of specified thickness. In each test, pressure transients were recorded using a digital oscilloscope (Tektronix, Beaverton, OR, USA). From each pressure recording at the tube exit, we computed the average and standard deviations for peak overpressure, impulse, and duration of the pressure transient (Table 2, Supplementary Fig. S1).

Blast injury

We weighed each animal prior to exposure of a mixed inhalation anesthetic of 3.5% isoflurane and 60% FiO_2 in an anesthetic induction chamber for 5 min. We confirmed anesthetic depth using a toe pinch. We then transferred the animal to the blast tube apparatus and placed it on the platform in the prone position. After securing the nose within the nose cone and encasing the torso in the sorbothane-lined aluminum encasing, we fired the blast tube, exposing the animal to a shockwave of predetermined pressure wave intensity. The peak overpressure ranged from 224 to 487 kPa. For sham conditions, we exposed the animal to identical anesthetic conditions, placed it in the blast tube apparatus for approximately the same period as pressure-exposed animals, and then placed it in the recovery cage.

Immediate neurological impairment

Immediately following injury, we carefully removed each animal from the blast apparatus and placed it in the original cage in the supine position. We closely observed each animal until the time of death or time of the end-point at 30 min post-injury. We measured immediate apnea as the time from the animal was placed in the supine position to the time the animal resumed breathing. To measure the righting reflex, or the righting time, we recorded the time the animal took to turn from the supine to prone position. If the animal resumed breathing post-injury but became apneic within the 30-min observation period, we recorded this finding as secondary apnea. We also recorded the presence and duration of dyspnea, or irregular breathing. To compare the righting times across the strains, we normalized the righting time of each injured animal with the average righting time for the sham animals within the respective strain. We compared the resulting measure, normalized righting time, across the strains.

Lethal-dose 50

To determine the thresholds for lethality, we exposed six animals of each strain to a blast peak overpressure beginning at 224 kPa. If >50% of animals survived in a given group, we incrementally increased the subsequent cohorts until lethality was observed within 30 min post-injury. We monitored the animals for 30 min post-injury and defined the parameters for lethality post-injury as death occurring within this window. We scored survival as a binary outcome (0 = survived 30 min post-injury; 1 = died within 30 min post-injury). Lethal-dose 50 (LD50) values were calculated using logistic regression based on the relationship between the peak overpressure and lethality rate for each strain.

Perfusion

At the time of death or 30 min post-bTBI, we gave each animal a lethal dose of pentobarbital sodium injection, USP, 250 mg/kg (Sagent Pharmaceuticals, Schaumburg, IL, USA) intraperitoneally (IP). When the animal was unresponsive to a toe pinch, we transcardially perfused it with 10 mL of ice-cold phosphate buffered saline and 25 mL of 10% neutral buffered formalin solution (Sigma-

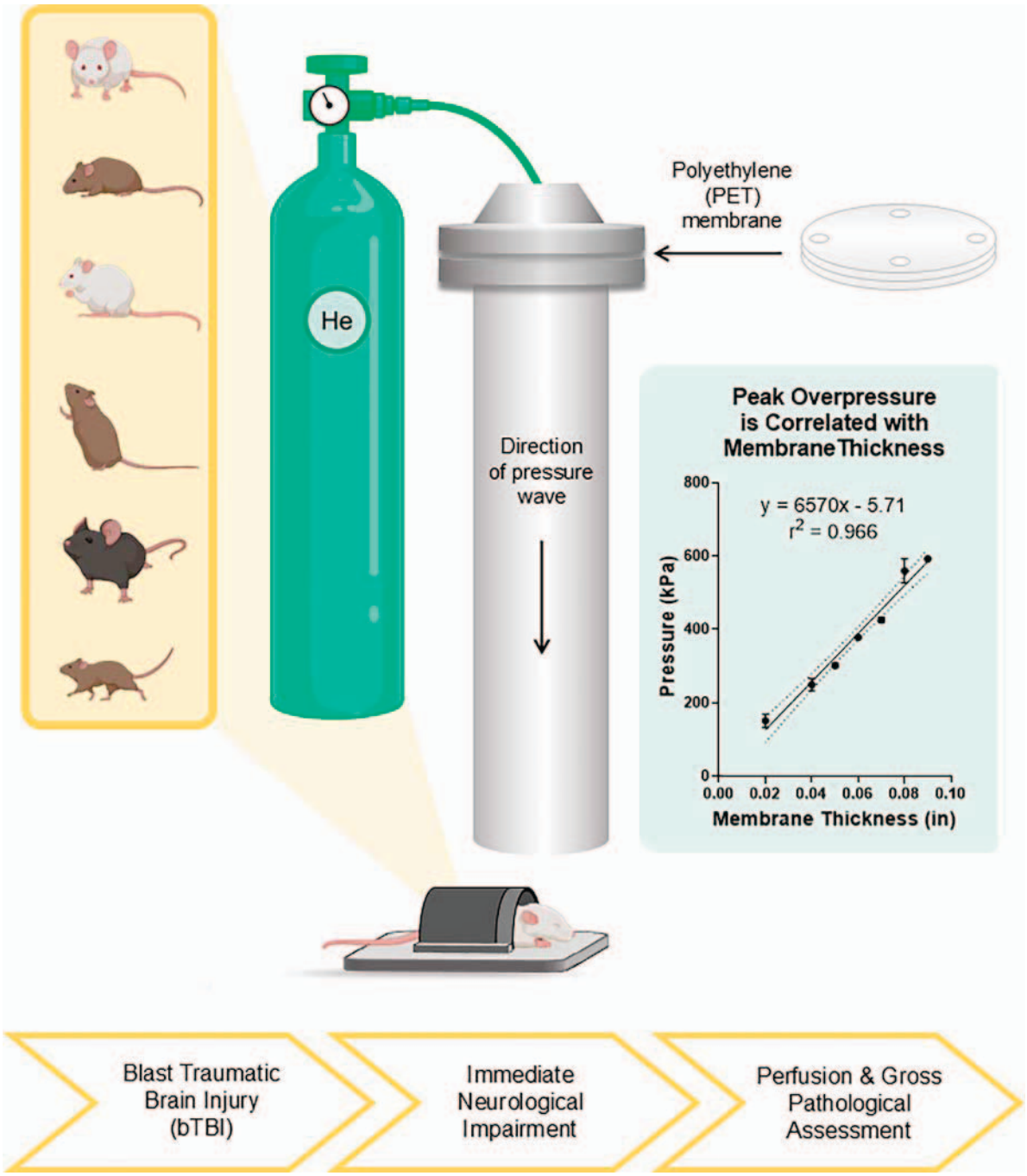

FIG. 1. Experimental schematic of bTBI. Blast tube apparatus representative of the peak overpressure wave generated by helium gas bursting through a PET membrane. Following bTBI, immediate neurological impairment assessment (apnea, dyspnea, righting time), gross pathological assessment, perfusion, and further histological analyses. Created in BioRender. Georges, A. (2025) https://BioRender.com/bk34l1p. bTBI, blast-induced traumatic brain injury; PET, polyethylene.

Table 2. Pressure, Impulse, and Duration of Peak Overpressure Wave

Membrane thickness (in)	*Peak overpressure (kPa)*	*Duration (msec)*	*Impulse (kPa*msec)*
0.02	150 ± 19	0.47 ± 0.008	10 ± 0.34
0.04	249 ± 17	0.74 ± 0.008	26 ± 1.93
0.05	301 ± 6	0.80 ± 0.011	35 ± 0.17
0.06	378 ± 1	0.88 ± 0.023	45 ± 0.22
0.07	429 ± 7	0.89 ± 0.051	53 ± 3.30
0.08	559 ± 32	0.95 ± 0.008	69 ± 4.09
0.09	592[a]	0.97[a]	75[a]

[a]No SD measurements for 0.09 in membrane thickness because only one pressure transducer measurement was obtained.

Polyethylene terephthalate (PET) membrane thickness, peak overpressure measurement, duration, and impulse as calculated from the pressure transducer measurements.

Data are shown as mean ± SD, $n = 3$.

Additional measurements and graphs shown in Supplementary Figure S1.

Aldrich, St. Louis, MO, USA) using a peristaltic pump (Avantor, Radnor, PA, USA) at a rate of 6 mL/min.

Gross pathology

Following perfusion, we dissected and examined the relevant organs for gross pathological changes. We grossly photographed the brain and lungs from each animal and scored pathologically on a scale using three categorical rankings. For the brain tissue rating scale, we defined: 0—brain tissue appeared healthy, with no visible gross pathology, bleeding, or damage; 1—bleeding at the brainstem, spinal cord, and/or cerebellum; and 2—subdural hematoma. For the lung tissue rating scale, we rated: 0—lung tissue appeared healthy, with no visible gross pathology, bleeding, or damage; 1—some signs of erythema or bleeding on the lungs, visible, healthy lung tissue; and 2—no visible healthy lung tissue, significant erythema, and bleeding into the chest cavity. We post-fixed all organs in 10% formalin for 24 h and recorded the weight of each brain.

Histology

We sectioned 8-μm-thick coronal sections between bregma 0 and 1.5 mm for each animal using a rotary microtome (Thermo Shandon Finesse 325 Rotary Microtome, Thermo Fisher, Waltham, MA, USA). We used hematoxylin and eosin staining to assess ventriculomegaly and abnormal neuropathology. To measure the ventricle size for each specimen, we captured a 4× image on a microscope system (Aperio ScanScope CS2, Leica Biosystems, Deer Park, IL, USA). After saving the images, we encircled each animal's left and right ventricles and measured their respective areas using ImageJ software.[52]

Statistical analysis

We performed all data analyses and created all graphs using Prism (GraphPad Software, Boston, MA, USA). We normalized the righting time outcomes at a consistent peak overpressure level (224 kPa) with respect to the group sham mean values. We analyzed the data presented in bar graphs nonparametrically using the Kruskal–Wallis test, followed by the *post hoc* test with Dunn's multiple comparisons as a result of a significant Shapiro–Wilk test for normality and a Brown–Forsythe test for unequal variance. We fit simple logistic regressions to determine the thresholds for the delayed righting time, immediate apnea, and lethality. From each logistic regression curve, we plotted and analyzed 95% confidence intervals (CIs) of the 50% risk level using an ordinary one-way ANOVA with uncorrected Fisher's least significant difference. All the error bars and ±values reported denote standard deviation. We determined significance by $p \leq 0.05$ and denoted significance as follows: ns $p > 0.05$, $^{*}p \leq 0.05$, $^{**}p \leq 0.01$, $^{***}p \leq 0.001$, $^{****}p \leq 0.0001$.

Results

Body weight and brain weight varied across genetic strains

The six genetic strains had unique physical appearances. Additionally, body weight differed significantly across strains (Kruskal–Wallis test, $p < 0.0001$). Over the same age ranges (8–10 weeks old), the NZO/HILtJ strain had significantly higher body weights than all the other strains (44.3 ± 4.4 g). CAST/EiJs had lower body weights (15.6 ± 1.2 g) (Fig. 2A,B). Across all strains, the brain weights varied slightly, but not significantly (Kruskal–Wallis test, $p < 0.0001$) (Fig. 2C, D). We next looked at the ratio of the brain weight to body weight across the strains (Kruskal–Wallis test, $p < 0.0001$). The NZO/HILtJ strain had the lowest brain/body weight ratio (0.011 ± 0.00096 g/g), while the CAST/EiJ strain had the highest brain/body weight ratio (0.025 ± 0.0021 g/g) (Fig. 2E,F).

Righting reflex is strain-dependent and significantly different between sham and bTBI conditions

To assess immediate neurological impairment, we measured the righting reflex, or the righting time, of each mouse following exposure to a peak overpressure wave. The righting reflex has been used in prior work

as an indicator of immediate neurological impairment.[54] We observed differences in the righting reflex in animals exposed to sham conditions across the strains. For this reason, we compared the normalized righting times across the strains exposed to the same blast pressure pulse (224 kPa peak, 22.4 kPa*msec impulse, 0.651-msec duration). The righting times, normalized to the mean sham righting time of each respective strain, varied significantly across the strains (Kruskal–Wallis test, $p < 0.0001$). When ranked by the duration of the normalized righting times, the *post hoc* analysis showed that the C57BL/6J strain (7.73 ± 4.88) had significantly greater normalized righting times than most other strains (NZO/HILtJ, 2.52 ± 1.77, $p = 0.0099$; NOD/ShiLtJ, 3.44 ± 2.07, $p = 0.0052$; 129S1/SvlmJ, 2.92 ± 1.70, $p = 0.0015$; CAst/EiJ, 1.64 ± 1.04, $p = 0.0003$) (Fig. 3A,B).

We next considered how the immediate neurological impairment varied with the blast overpressure level. Logistic regression analysis on animals exposed to a range of overpressure conditions showed that the genetic strain was a significant factor in the range of the righting times observed (ANOVA, $p < 0.0001$). *Post hoc* comparison across strains revealed two distinct, nonoverlapping groups in normalized righting times. Group 1 consisted of NZO/HILtJ (298 ± 179), NOD/ShiLtJ (279 ± 152), and C57BL/6J (267 ± 158), which required higher peak overpressures to induce prolonged righting times. Group 2 consisted of A/J (161 ± 186), 129S1/SvlmJ (159 ± 176), and CAst/EiJ (82.3 ± 185), which had lower thresholds for prolonged righting times. Both groups were significantly different from sham exposure levels (Fig. 3C,D).

Strain-dependent differences in respiratory symptoms occurred over a range of blast overpressure exposures

To explore the relationship between blast exposure and pulmonary damage, we considered the acute (<30 min) response to blast overpressure. For all overpressure levels (224–487 kPa), most strains showed normal respirations and respiratory rates in the majority of cases (>50%). The exceptions being the A/J and CAST/EiJ strains, showing respiratory impairments post-injury in 51.4% and 52.2% of cases, respectively. The A/J strain had the highest percentage of cases with dyspnea (17.1%), and the NOD/ShiLtJ had the lowest (3.5%). The CAST/EiJs had the most frequent instances of immediate apnea (47.8%) but no instances of delayed apnea. The percentage of cases with delayed apnea post-blast was minimal across the strains, but the most prevalent was in the 129S1/SvlmJ (7.02%) and NZO/HILtJ (4.08%) strains (Fig. 4A).

We considered if the overpressure threshold for immediate respiratory apnea following bTBI was different across the strains. After separating the response into either the presence (=1) or absence (=0) of apnea, we plotted the 95% CIs of each strain and determined that there was a significant relationship between the genetic background and apnea threshold (one-way ANOVA, $p = 0.0018$). The NOD/ShiLtJ (468 ± 210 kPa) and NZO/HILtJ (444 ± 498 kPa) strains have the highest thresholds of the peak overpressure level for immediate apnea, which were not different from one another (ns, $p = 0.492$) (Fig. 4B). *Post hoc* testing showed that the NOD/ShiLtJ and NZO/HILtJ strains also had significantly higher thresholds than the A/J strain (275 ± 132, $p = 0.0262$, $p = 0.0065$, respectively). The CAST/EiJ (207 ± 339 kPa) strain was significantly more susceptible to immediate apnea at lower blast levels than most of the other strains (NOD/ShiLtJ, $p = 0.0009$; NZO/HILtJ, $p = 0.0002$; 129S1/SvlmJ [395 ± 213], $p = 0.0084$; C57BL/6J [369 ± 376], $p = 0.0109$) (Fig. 4C,D).

Lethality thresholds were also strain-dependent

To determine whether the genotype was a contributing factor to the lethality of a particular strain, we established LD50 thresholds for each of the six strains of mice. Broadly, a genetic strain was a significant factor in the blast overpressure needed to achieve 50% likelihood of lethality. The LD50 values, ranked from most susceptible to least susceptible strain, were: CAST/EiJ (200 ± 245 kPa), A/J (310 ± 155 kPa), 129S1/SvlmJ (390 ± 154 kPa), C57BL/6J

FIG. 2. Six genetic strains, body mass, and brain mass. The six genetically diverse mouse strains and their profile images from the Jackson Laboratory.[53] **(A)** Body weight across the mouse strains. **(B)** Heatmap of *p* values after the Kruskal–Wallis test, followed by *post hoc* Dunn's multiple comparisons test of body weight across the strains. **(C)** Brain weight across the mouse strains. **(D)** Heatmap of *p* values after the Kruskal–Wallis test, followed by *post hoc* Dunn's multiple comparisons test of brain weight across the strains. **(E)** Brain/body weight ratio across the mouse strains. **(F)** Heatmap of *p* values after the Kruskal–Wallis test, followed by *post hoc* Dunn's multiple comparisons test of brain/body weight ratio across the strains. Purple: $p \leq 0.05$, gray: $p > 0.05$.

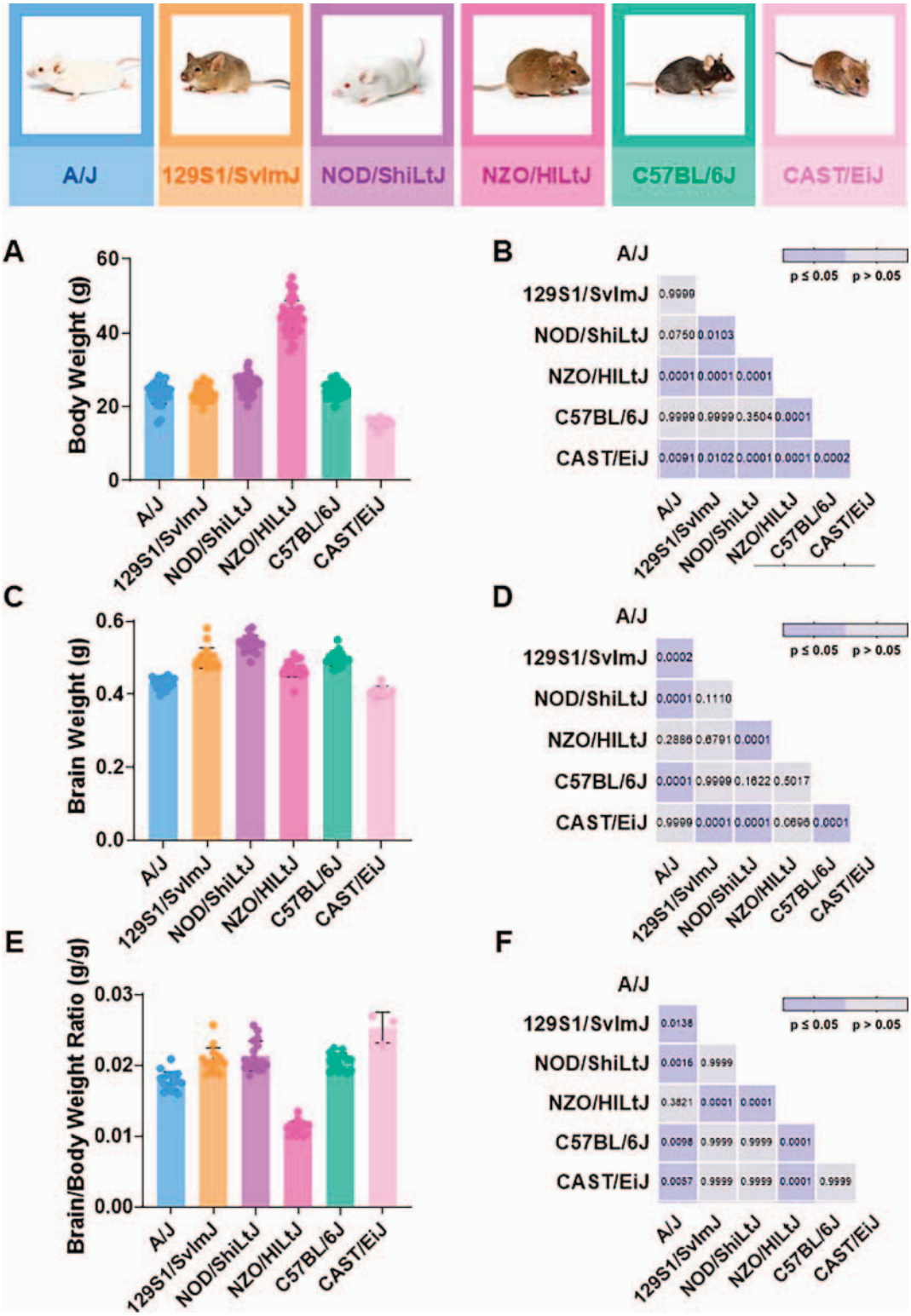
A/J
129S1/SvImJ
NOD/ShiLtJ
NZO/HILtJ
C57BL/6J
CAST/EiJ
A
Body Weight (g)
60
40
20
0
B
p ≤ 0.05
p > 0.05
129S1/SvImJ 0.9999
NOD/ShiLtJ 0.0750 0.0103
NZO/HILtJ 0.0001 0.0001 0.0001
C57BL/6J 0.9999 0.9999 0.3504 0.0001
CAST/EiJ 0.0091 0.0102 0.0001 0.0001 0.0002
C
Brain Weight (g)
0.6
0.4
0.2
0.0
D
p ≤ 0.05
p > 0.05
129S1/SvImJ 0.0002
NOD/ShiLtJ 0.0001 0.1110
NZO/HILtJ 0.2886 0.6791 0.0001
C57BL/6J 0.0001 0.9999 0.1622 0.5017
CAST/EiJ 0.9999 0.0001 0.0001 0.0696 0.0001
E
Brain/Body Weight Ratio (g/g)
0.03
0.02
0.01
0.00
F
p ≤ 0.05
p > 0.05
129S1/SvImJ 0.0138
NOD/ShiLtJ 0.0016 0.9999
NZO/HILtJ 0.3821 0.0001 0.0001
C57BL/6J 0.0098 0.9999 0.9999 0.0001
CAST/EiJ 0.0057 0.9999 0.9999 0.0001 0.9999

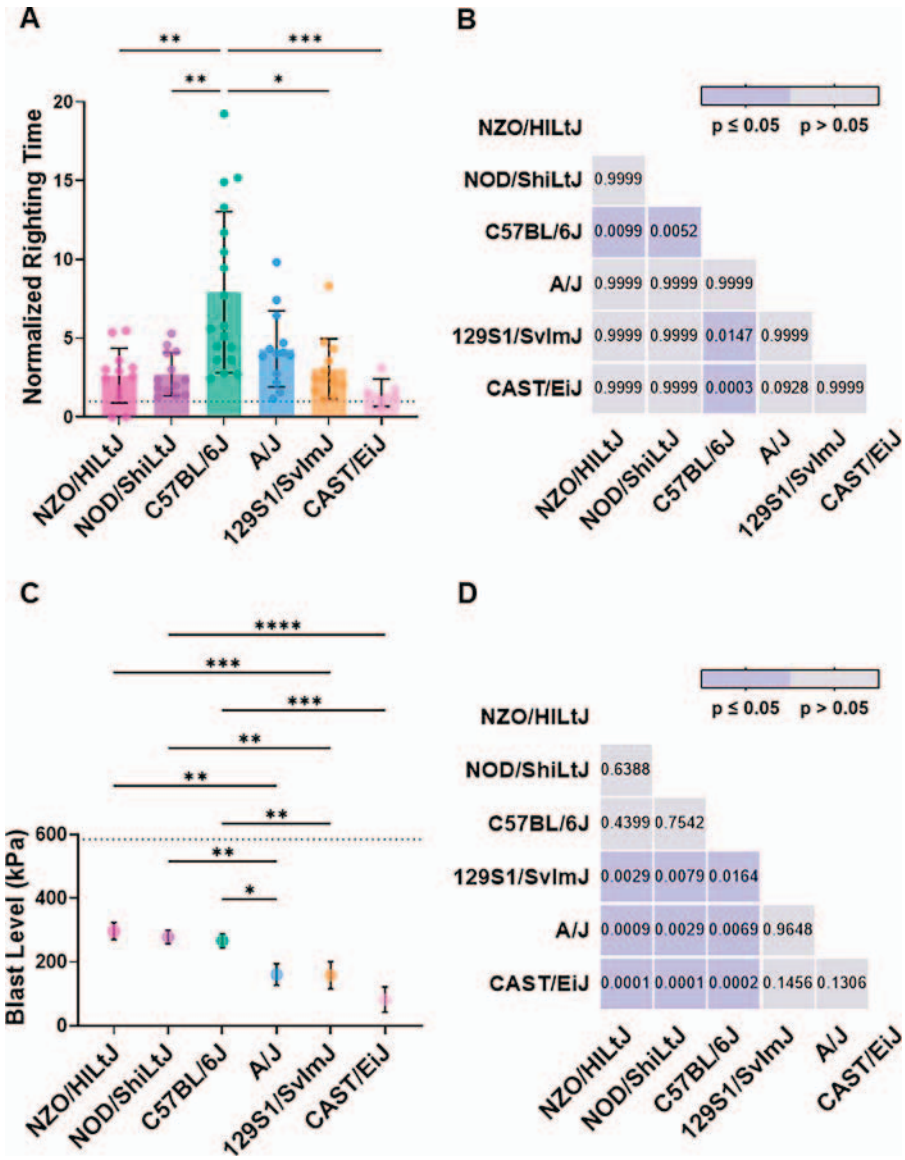

FIG. 3. Immediate neurological impairment following bTBI. **(A)** Normalized righting times across the strains at a consistent blast level of 224 kPa. Data are shown as x at mean ± SD. **(B)** Heatmap of the Kruskal–Wallis multiple comparisons test for the normalized righting times. **(C)** x at 50% (blast level causing 50% prolonged righting time in each strain) across the strains. Data are presented as mean ± 95% CI. **(D)** Heatmap of one-way ANOVA with uncorrected Fisher's LSD multiple comparisons test for data in C. Purple: $p \leq 0.05$, gray: $p > 0.05$. bTBI, blast-induced traumatic brain injury.

(429 ± 155 kPa), NZO/HILtJ (474 ± 347), and NOD/ShiLtJ (517 ± 272 kPa) (Fig. 5A). *Post hoc* comparisons of the 50% CIs of LD50 thresholds show that the NOD/ShiLtJ and NZO/HILtJ strains showed the highest resilience to injury, and these thresholds were not different from each other (ns, $p = 0.8349$). Moreover, the threshold for CAST/EiJs was significantly less than all the other strains (NOD/ShiLtJ, NZO/HILtJ, C57BL/6J, 129S1/SvImJ, $p < 0.0001$; A/J, $p = 0.0054$). The NOD/ShiLtJ thresholds were significantly higher than most of the other strains (C57BL/6J, $p = 0.0297$; 129S1/SvImJ, $p = 0.066$; A/J, $p = 0.0003$; CAST/EiJ, $p < 0.0001$).

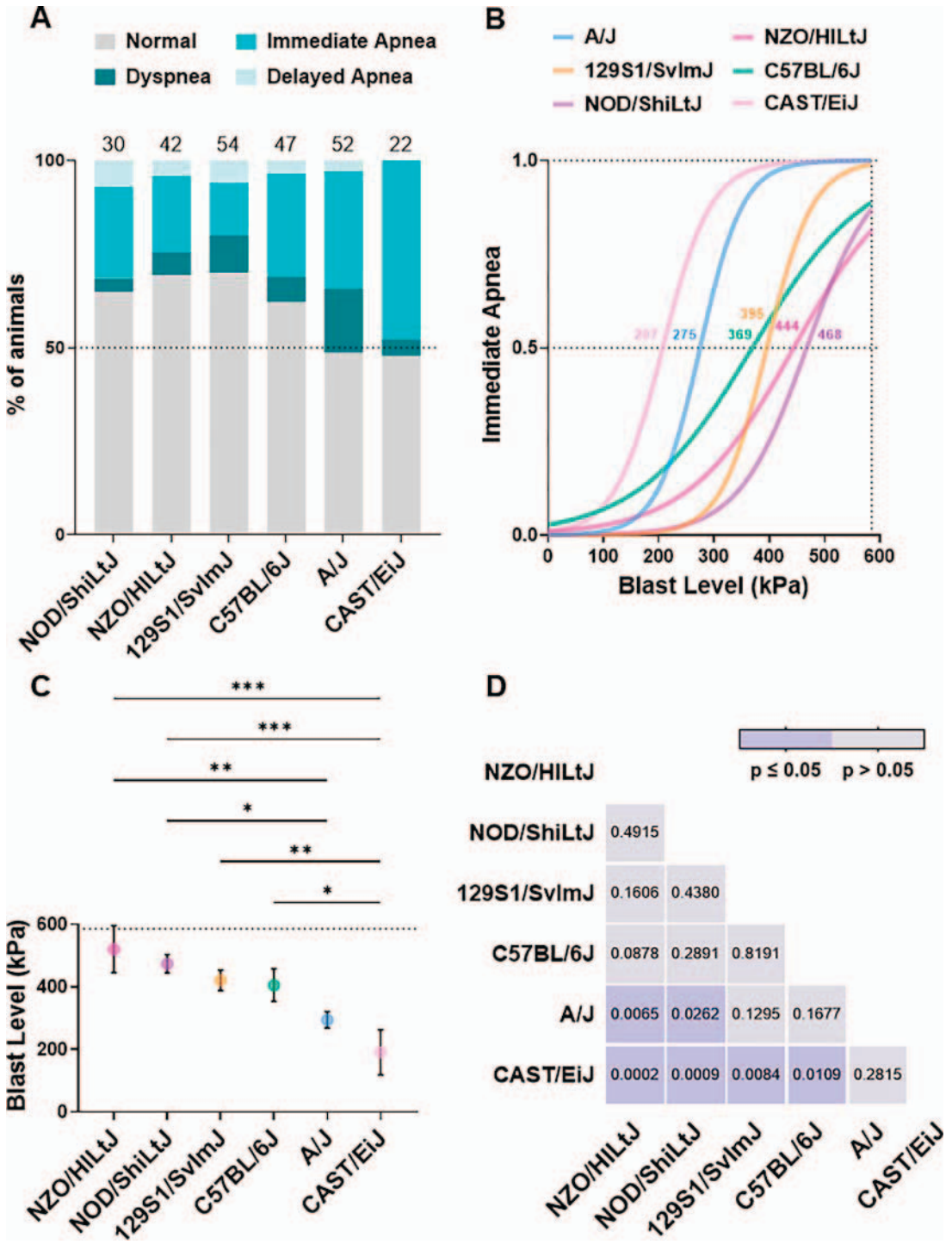

FIG. 4. Respiratory symptoms following bTBI. **(A)** Respiratory symptoms following bTBI. Data shown as percent of animals. **(B)** Primary apnea logistic regression across all blast levels (0–487 kPa). Absence of primary apnea (=0) and presence of primary apnea (=1). **(C)** x at 50% (blast level causing 50% primary apnea in each strain) across the strains. Data are presented as mean ± 95% CI. **(D)** Heatmap of one-way ANOVA with Fisher's uncorrected LSD multiple comparisons test. Purple: $p \leq 0.05$, gray: $p > 0.05$. bTBI, blast-induced traumatic brain injury.

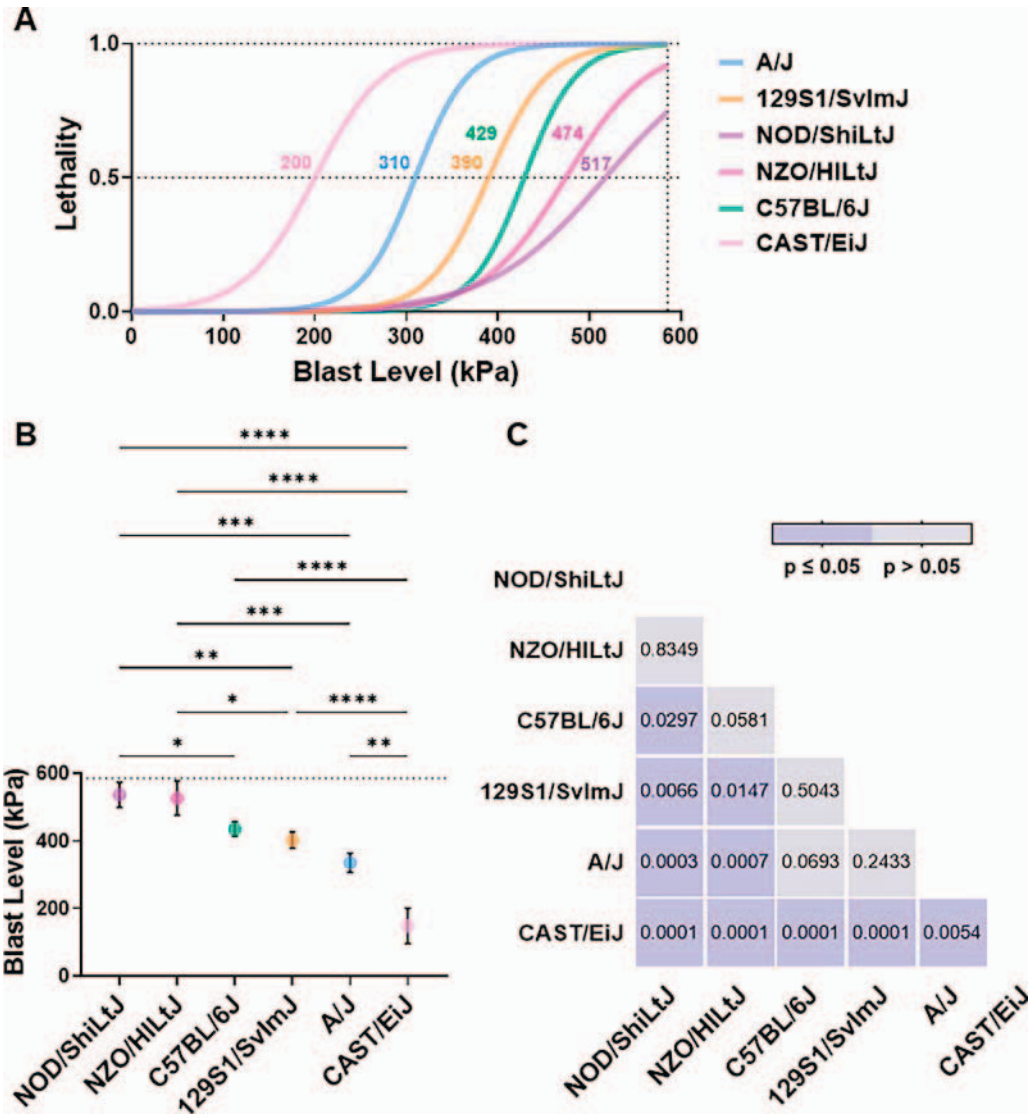

FIG. 5. Thresholds for lethality. **(A)** Lethality logistic regression across all blast levels (0–487 kPa). Died following bTBI (=0) and survived following bTBI (=1). **(B)** LD50 values across all blast levels (0–487 kPa). Data are presented as mean ± 95% CI. **(C)** Heatmap of one-way ANOVA with uncorrected Fisher's LSD multiple comparisons test. Purple: $p \leq 0.05$, gray: $p > 0.05$. LD50, lethal-dose 50.

C57BL/6Js do not have significantly different lethality thresholds than the NZO/HILtJs ($p = 0.0581$), 129S1/SvImJs ($p = 0.5043$), or A/Js ($p = 0.0693$) (Fig. 5B,C).

Gross brain and lung lesions after blast overpressure differed with genetic background

Given the difference in the lethality thresholds, we next examined if there were distinct patterns of primary blast and lung injuries across genetic strains. Using a semi-quantitative scoring method for the primary brain pathology appearing after blast exposure, we observed a considerable difference in the type and frequency across genetic strains. Subdural hematoma is one primary type of brain bleeding that appears after blast loading,[55,56] and C57BL/6Js had the highest incidence of subdural brain hematoma (71.42%). In contrast, the NZO/HILtJs had no subdural bleeding (Fig. 5A). In both the A/Js and CAST/EiJs, more than half of the animals had some type

of primary cerebral pathology in fatal cases. The NOD/ShiLtJ strain had the fewest cases of macroscopic cerebral bleeding (80% with no gross cerebral pathology) (Fig. 6A).

Similar to the primary brain pathology observations, the type and incidence of pulmonary changes varied considerably across the genetic strains. Macroscopic pulmonary bleeding was observed in 80% of the NZO/HILtJs following a lethal bTBI. In contrast, both the C57BL/6J and CAST/EiJ strains had no observable pulmonary damage. The results were mixed with the A/J and 129S1/SvlmJ stains, with ≥50% of fatal cases with no observable pulmonary damage and some cases in each group with mild and severe pulmonary damage (Fig. 6B).

Brain histology and cerebral bleeding varied across genetic strains following bTBI at respective LD50 levels

Across the strains and within individual strains, we observed significantly different patterns of primary cerebrovascular lesions (Fig. 7A). Subarachnoid hemorrhage (SAH) was the most common across all animals blasted at their respective LD50 levels, regardless of the genetic strain. Intraparenchymal hemorrhage

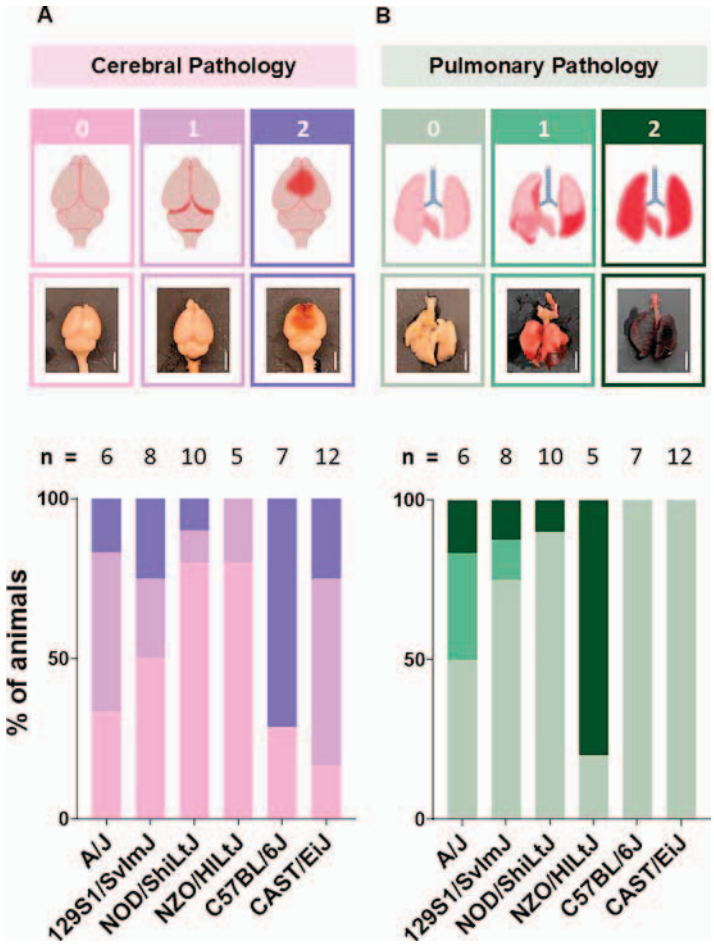

FIG. 6. Gross cerebral and pulmonary pathology. **(A)** Gross brain pathology scoring: 0—no visible gross pathology, 1—bleeding at brainstem, spinal cord, and/or cerebellum, 2—subdural hematoma. Figure created with Biorender. **(B)** Gross lung pathology scoring: 0—no visible gross pathology, 1—some signs of erythema or bleeding, 2—significant erythema and bleeding. Observed in animals that died following bTBI. Data represented as percentage of animals. Scale bar = 500 μm. bTBI, blast-induced traumatic brain injury. Created in BioRender. Georges, A. (2025) https://BioRender.com/5x0uczm

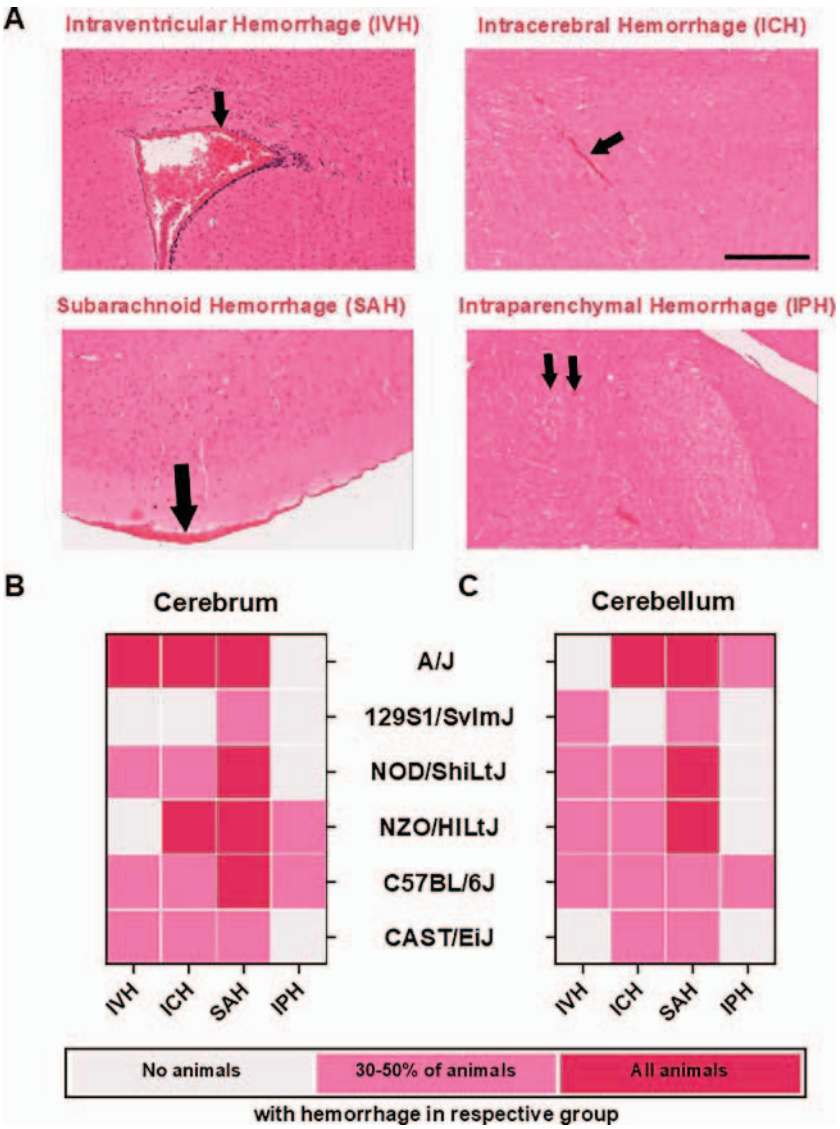

FIG. 7. Histological cerebral pathology. **(A)** Types of cerebral bleeding and representative microscopic images from coronal slice following H&E staining. Arrows pointing toward identified areas of bleeding. Scale bar = 60 μm. **(B)** Presence/absence of each type of hemorrhage in the cerebrum. **(C)** Presence/absence of each type of hemorrhage in the cerebellum. n = 3 per group.

(IPH) was the least common, observed only in a subset of animals; in the C57BL/6J strain, IPH was in the cerebrum and cerebellum; in the NZO/HILtJ strain, IPH was only in the cerebrum; in the A/J strain, we only observed IPH in the cerebellum. Intraventricular hemorrhage (IVH) and intracranial hemorrhage (ICH) had mixed occurrences. Notably, the A/J strain had the highest frequency of microscopic hemorrhage, as all animals had ICH and SAH in both the cerebrum and cerebellum, and all animals had IVH in the cerebrum (Fig. 7B,C). A preliminary examination of the ventricular size at LD50 levels showed that the strain (p = 0.0039), rather than blast exposure, was a more relevant factor to explain the changes in the ventricular size (Supplementary Fig. S2).

Discussion

Our study characterized the responses of six distinct murine genetic strains to bTBI, revealing significant

strain-specific differences in the righting times, respiratory symptoms, lethality thresholds, and gross pathological changes. Broadly, these findings highlight the substantial role of the genetic background in the acute response and outcome to blast exposure. Among the most striking results were the unexpected resilience of the NOD/ShiLtJ (T1DM) and NZO/HlLtJ (T2DM) strains to blast injury, implying that brain metabolism homeostasis and immune system state may play a particularly important role in the acute effects of blast TBI.

We observed substantial strain-dependent differences in multiple outcome measures, suggesting the involvement of biophysical, genetic, or other factors in the response to blast injury. The C57BL/6J strain, serving as a baseline, had significantly longer righting times and the highest susceptibility to subdural hematomas. The A/J strain was the most susceptible to dyspnea and had a lower apnea threshold, while the 129S1/SvlmJ strain showed similar responses to C57BL/6J. The CAST/EiJ strain was the most susceptible to lethality at lower blast levels, possibly related to their smaller body size.

One potential explanation for these differences across the strains could be the physical characteristics, such as skull shape, brain size, and vasculature differences across the strains. For acceleration-induced injuries, there is a clear consensus that differences across the brain size and shape, and even their network structure, should be accounted for when considering injury risk.[57–60] Although we observed changes in the brain size across the strains, the proposed scaling relationships for blast loading[57,61] do not fully explain the differences in lethality that we observed across the strains. For example, the largest brain sizes did not show the lowest LD50 threshold, and the smallest sizes did not show the highest threshold. In addition, it is possible that other physical features may also affect the lethality thresholds or immediate neurological impairment. For example, computational models suggest that skull properties play a crucial role in the transmission of blast waves to the brain.[51,52,60,62] Similarly, the skull shape exposed to the incident blast wave may also affect the reflection and transmission of the shock wave. The NZO/HlLtJ strain has a characteristically flat skull relative to other strains.[63] This flatter skull geometry may influence blast-wave reflection, potentially explaining the increased resilience to blast exposure observed in this strain. Both the physical properties and geometric shapes of the skull are not well-defined across these strains and would require a more precise characterization before determining the relative role that each plays in transmitting a blast wave into the brain parenchyma.

While we cannot rule out physical factors, genetic variations among the strains may also contribute to the observed differences in outcome. For example, the A/J strain's susceptibility to lung diseases[25] could relate to their vulnerability to respiratory symptoms post-bTBI. Alternatively, past work shows that the *Muc5b* gene, associated with lung inflammation and fibrosis, is highly expressed in NZO/HlLtJ and minimally expressed in CAST/EiJ,[64] aligning with our gross pathology findings, which showed that primary lung damage was more apparent in the NZO/HlLtJ strain than other strains.

Perhaps the most intriguing observation from our dataset is the resilience of the NOD/ShiLtJ and NZO/HlLtJ strains to blast injury. On its own, the NOD/ShiLtJ mouse's autoimmune predisposition makes it a worthwhile candidate for studying post-TBI autoimmunity given the substantial clinical evidence of autoantibody production after TBI. Clinical studies have documented diverse autoantibody responses following TBI, including antibodies against *GFAP*,[65,66] *S100B*,[67] and neural antigens such as *MAG*.[68] The NOD/ShiLtJ mouse's defects in central tolerance and abnormal T-cell responses mirror mechanisms implicated in human post-TBI autoimmunity, where the blood–brain barrier (BBB) disruption exposes normally sequestered neural antigens to the immune system.[67,69] Both clinical data and animal models suggest that repeated TBI exposures lead to more pronounced autoimmune responses,[65] while $CD8^+$ T cells appear to play a key pathogenic role in chronic neurodegeneration after TBI.[70] Indeed, reports of the BBB compromise and subsequent activation of the immune system and inflammatory pathways after blast exposure are now appearing in the literature and may make the NOD/ShiLtJ strain even more relevant for examining the relationship between autoimmunity and blast TBI.[71–74] The baseline immune dysregulation in NOD/ShiLtJ mice, which includes impaired antigen-presenting cell function and abnormal natural killer cell responses, could clearly affect the course of recovery after blast exposure.

In comparison, the NZO/HlLtJ (New Zealand Obese) mouse provides a relevant model for studying TBI outcomes in diabetic patients due to its polygenic obesity and the spontaneous development of type 2 diabetes with associated chronic inflammation.[65,75] Clinical

studies demonstrate that diabetes is an independent risk factor for worse outcomes after TBI, including increased mortality (hazard ratio (HR): 1.89, 95% CI: 1.4–2.6),[76,77] and is associated with greater neuroinflammation[73] and impaired functional recovery.[76,78] The NZO mouse's phenotype of early-onset obesity, progressive insulin resistance, and chronic low-grade inflammation[77,79] mirrors key pathophysiological mechanisms seen in human diabetic patients who experience worse outcomes after TBI.[75] Moreover, diabetic patients show higher rates of neurodegenerative complications post-TBI,[80] making the NZO mouse's metabolic phenotype particularly relevant for studying the intersection of diabetes, inflammation, and poor neurological recovery after brain injury.

Several limitations should be considered when interpretating these findings. First, this study exclusively used male mice, which may limit generalizability given the known sex differences in TBI outcomes and neuroinflammatory responses. Additionally, all consisted of age-matched adult mice evaluated at a single acute end-point (30 min post-injury), precluding the assessment of sex-specific, age-dependent, or temporal evolution of blast-induced pathology. These constraints highlight the need for future studies examining female mice, varying ages, and multiple time points to fully characterize the genetic determinants of blast-induced TBI outcomes.

Our data from all evaluated founder strains demonstrate the substantial influence of genetic background on acute bTBI response and outcome in mice. The intriguing resilience of diabetic strains to blast injury, despite their metabolic status, highlights the complex interplay between genetics, immune function, brain metabolism, and blast tolerance. Much like how the collaborative crossing of founder strains identified gene loci responsible for vascular network differences, which could underlie stroke impairment,[81] bone remodeling after hind limb unloading,[82] and DNA damage after ionizing radiation,[83] these observations provide a path to produce a collaborative crossing of founder strains to better pinpoint the possible genetic origins of the different outcomes observed after blast exposure. As some of the genetic strains may be better suited to study the long-term effects of TBI, our results will aid in guiding these studies by characterizing the thresholds and acute responses for a range of loading conditions. Ultimately, a better understanding of these genetic influences could guide the development of personalized therapies and improve the prevention and management of blast-induced neurotrauma. Additionally, future research should aim to link post-injury findings with specific gene loci and explore how genetic factors influence the outcomes across the spectrum of blast injuries, from single high-magnitude exposures to multiple subconcussive exposures.

Transparency, Rigor, and Reproducibility Statement

All animal procedures were conducted according to the protocols approved by Institutional Animal Care and Use Committees (IACUC) at both the University of Pennsylvania and the CMC VAMC. To study the lethality thresholds of each genetic strain, we started at low peak overpressure levels, in which we presumed 100% of the animals would survive. We incrementally increased the peak overpressure that we exposed each animal to in order to minimize the blast pressure needed to complete the logistic regression curves. To confirm the validity of our calculated lethality thresholds, in another cohort, we enrolled each strain (n = 12) at their respective LD10 levels. Approximately 10% of animals of the A/J, NOD/LtJ, NZO/HlLtJ, C57BL/6J, and CAST/EiJ strains died immediately post-injury, confirming our results. The exception was the 129S1/SvImJ strain—30% died at the precalculated LD10 level. We added the additional lethality data to our logistic regression plots, and all strain LD50 levels remained the same, except the 129S1/SvImJ LD50 decreased. This verified our results and increased the accuracy of the 129S1/SvImJ lethality data. An experimenter blinded to the strain and condition of each animal analyzed the brain histology.

Acknowledgments

The authors are grateful to Kathryn R. Jacobson, Adam C. Rayfield, and Erin D. Anderson for editorial review and comments.

Authors' Contributions

A.P.G.: Conceptualization, methodology, data analysis, figures, writing. K.D.B.: Conceptualization, methodology, writing—review and editing. D.V.A. and A.H.B.: Methodology, data analysis. D.K.C.: Supervision, conceptualization, funding acquisition. D.F.M.: Supervision, conceptualization, funding acquisition, writing.

Funding Information

This material is based upon work generously supported by the Department of Veterans Affairs, Office

of Research and Development through Merit Review I01-BX005017 (PI: D.K.C.).

Author Disclosure Statement

No competing financial interests exist.

Supplementary Material

Supplementary Figures

References

1. Terrio H, Brenner LA, Ivins BJ, et al. Traumatic brain injury screening: Preliminary findings in a US Army Brigade Combat Team. J Head Trauma Rehabil 2009;24(1):14–23; doi: 10.1097/HTR.0b013e31819581d8
2. Covington NV, Duff MC. Heterogeneity is a hallmark of traumatic brain injury, not a limitation: A new perspective on study design in rehabilitation research. Am J Speech Lang Pathol 2021;30(2S):974–985; doi: 10.1044/2020_AJSLP-20-00081
3. Agoston D, Arun P, Bellgowan P, et al. Military blast injury and chronic neurodegeneration: Research presentations from the 2015 international state-of-the-science meeting. J Neurotrauma 2017;34(S1):S6–S17; doi: 10.1089/neu.2017.5220
4. Agoston DV. Modeling the long-term consequences of repeated blast-induced mild traumatic brain injuries. J Neurotrauma 2017;34(S1):S44–S52; doi: 10.1089/neu.2017.5317
5. Cernak I. The importance of systemic response in the pathobiology of blast-induced Neurotrauma. Front Neurol 2010;1:151; doi: 10.3389/fneur.2010.00151
6. Cernak I, Merkle AC, Koliatsos VE, et al. The pathobiology of blast injuries and blast-induced neurotrauma as identified using a new experimental model of injury in mice. Neurobiol Dis 2011;41(2):538–551; doi: 10.1016/j.nbd.2010.10.025
7. Tran TTT, Corsini S, Kellingray L, et al. APOE genotype influences the gut microbiome structure and function in humans and mice: Relevance for Alzheimer's disease pathophysiology. Faseb J 2019;33(7):8221–8231; doi: 10.1096/fj.201900071R
8. Harper MM, Boehme N, Dutca LM, et al. The retinal ganglion cell response to blast-mediated traumatic brain injury is genetic background dependent. Invest Ophthalmol Vis Sci 2021;62(7):13; doi: 10.1167/iovs.62.7.13
9. Zuckerman A, Siedhoff HR, Balderrama A, et al. Individualized high-resolution analysis to categorize diverse learning and memory deficits in tau rTg4510 mice exposed to low-intensity blast. Front Cell Neurosci 2024;18:1397046; doi: 10.3389/fncel.2024.1397046
10. Jackson M, Chen S, Nguyen TT, et al. The chronic effects of a single low-intensity blast exposure on Phosphoproteome networks and cognitive function influenced by mutant tau overexpression. Int J Mol Sci 2024;25(6):3338; doi: 10.3390/ijms25063338
11. Consortium CC. The genome architecture of the collaborative cross mouse genetic reference population. Genetics 2012;190(2):389; doi: 10.1534/genetics.111.132639
12. Saul MC, Philip VM, Reinholdt LG, et al.; Center for Systems Neurogenetics of Addiction. High-diversity mouse populations for complex traits. Trends Genet 2019;35(7):501–514; doi: 10.1016/j.tig.2019.04.003
13. Svenson KL, Gatti DM, Valdar W, et al. High-resolution genetic mapping using the mouse diversity outbred population. Genetics 2012;190(2):437–447; doi: 10.1534/genetics.111.132597
14. Yang H, Wang X, Blanco-Gómez A, et al. A susceptibility gene signature for ERBB2-driven mammary Tumour development and metastasis in collaborative cross mice. EBioMedicine 2024;106:105260; doi: 10.1016/j.ebiom.2024.105260
15. Churchill GA, Gatti DM, Munger SC, et al. The diversity outbred mouse population. Mamm Genome 2012;23(9–10):713–718; doi: 10.1007/s00335-012-9414-2
16. Keele GR. Which mouse multiparental population is right for your study? The collaborative cross inbred strains, their F1 hybrids, or the diversity outbred population. G3 (Bethesda) 2023;13(4):jkad027; doi: 10.1093/g3journal/jkad027
17. Churchill GA, Airey DC, Allayee H, et al.; Complex Trait Consortium. The collaborative cross, a community resource for the genetic analysis of complex traits. Nat Genet 2004;36(11):1133–1137; doi: 10.1038/ng1104-1133
18. Xuan W, Zhang L, Zhang Y, et al. Genetic mapping of behavioral traits using the collaborative cross resource. Int J Mol Sci 2022;24(1):682; doi: 10.3390/ijms24010682
19. Leist SR, Pilzner C, van den Brand JM, et al. Influenza H3N2 infection of the collaborative cross founder strains reveals highly divergent host responses and identifies a unique phenotype in CAST/EiJ mice. BMC Genomics 2016;17:143; doi: 10.1186/s12864-016-2483-y
20. Schoenrock SA, Gagnon L, Olson A, et al. The collaborative cross strains and their founders vary widely in cocaine-induced behavioral sensitization. Front Behav Neurosci 2022;16:886524; doi: 10.3389/fnbeh.2022.886524
21. Soni N, Hohsfield LA, Tran KM, et al. Genetic diversity promotes resilience in a mouse model of Alzheimer's disease. Alzheimers Dement 2024;20(4):2794–2816; doi: 10.1002/alz.13753
22. Tryndyak VP, Willett RA, Avigan MI, et al. Non-alcoholic fatty liver disease-associated DNA methylation and gene expression alterations in the livers of collaborative cross mice fed an obesogenic high-fat and high-sucrose diet. Epigenetics 2022;17(11):1462–1476; doi: 10.1080/15592294.2022.2043590
23. Baban B, Braun M, Khodadadi H, et al. AMPK induces regulatory innate lymphoid cells after traumatic brain injury. JCI Insight 2021;6(1):e126766; doi: 10.1172/jci.insight.126766
24. Murray KE, Ravula AR, Stiritz VA, et al. Sex and genotype affect mouse hippocampal gene expression in response to blast-induced traumatic brain injury. Mol Neurobiol 2025;62(8):9980–10005; doi: 10.1007/s12035-025-04879-5
25. Crusio WE, Sluyter F, Gerlai RT, et al. eds. Behavioral genetics of the mouse. In: Cambridge Handbooks in Behavioural Genetics. Cambridge University Press: Cambridge ; New York; 2013.
26. Hamilton GF, Majdak P, Miller DS, et al. Evaluation of a C57BL/6J x 129S1/SvImJ hybrid nestin-thymidine kinase transgenic mouse model for studying the functional significance of exercise-induced adult hippocampal neurogenesis. Brain Plast 2015;1(1):83–95; doi: 10.3233/BPL-150011
27. Kluth O, Mirhashemi F, Scherneck S, et al. Dissociation of lipotoxicity and glucotoxicity in a mouse model of obesity associated diabetes: Role of Forkhead box O1 (FOXO1) in glucose-induced beta cell failure. Diabetologia 2011;54(3):605–616; doi: 10.1007/s00125-010-1973-8
28. Gao J, Killedar S, Cornelius JG, et al. Sjögren's syndrome in the NOD mouse model is an interleukin-4 time-dependent, antibody isotype-specific autoimmune disease. J Autoimmun 2006;26(2):90–103; doi: 10.1016/j.jaut.2005.11.004
29. Liao J, He Q, Huang Z, et al. Network pharmacology-based strategy to investigate the mechanisms of artemisinin in treating primary Sjögren's syndrome. BMC Immunol 2024;25(1):16; doi: 10.1186/s12865-024-00605-3
30. Steward CA, Humphray S, Plumb B, et al. Genome-wide end-sequenced BAC resources for the NOD/MrkTac☆ and NOD/ShiLtJ☆☆ mouse genomes. Genomics 2010;95(2):105–110; doi: 10.1016/j.ygeno.2009.10.004
31. Leiter EH. Selecting the "right" mouse model for metabolic syndrome and type 2 diabetes research. Methods Mol Biol 2009;560:1–17; doi: 10.1007/978-1-59745-448-3_1
32. Schaffenrath J, Huang S-F, Wyss T, et al. Characterization of the blood-brain barrier in genetically diverse laboratory mouse strains. Fluids Barriers CNS 2021;18(1):34; doi: 10.1186/s12987-021-00269-w
33. Ohlemiller KK, Rice MER, Gagnon PM. Strial microvascular pathology and age-associated endocochlear potential decline in NOD congenic mice. Hear Res 2008;244(1–2):85–97; doi: 10.1016/j.heares.2008.08.001
34. Ewing LE, Miousse IR, Pathak R, et al. NZO/HlLtJ as a novel model for the studies on the role of metabolic syndrome in acute radiation toxicity. Int J Radiat Biol 2020;96(1):93–99; doi: 10.1080/09553002.2018.1547437
35. Lisi V, Singh B, Giroux M, et al. Enhanced neuronal regeneration in the CAST/Ei mouse strain is linked to expression of differentiation markers after injury. Cell Rep 2017;20(5):1136–1147; doi: 10.1016/j.celrep.2017.07.010
36. Griesdale DEG, Tremblay M-H, McEwen J, et al. Glucose control and mortality in patients with severe traumatic brain injury. Neurocrit Care 2009;11(3):311–316; doi: 10.1007/s12028-009-9249-1

37. Leme AS, Berndt A, Williams LK, et al. A survey of airway responsiveness in 36 inbred mouse strains facilitates gene mapping studies and identification of quantitative trait loci. Mol Genet Genomics 2010;283(4): 317–326; doi: 10.1007/s00438-010-0515-x
38. Omura T, Omura K, Tedeschi A, et al. Robust axonal regeneration occurs in the injured CAST/Ei mouse CNS. Neuron 2016;90(3):662; doi: 10.1016/j.neuron.2016.04.025
39. Axelsson H, Yelverton JT. Chest wall velocity as a predictor of nonauditory blast injury in a complex wave environment. J Trauma 1996;40 (3 Suppl):S31–S7; doi: 10.1097/00005373-199603001-00006
40. Bass CR, Rafaels KA, Salzar RS. Pulmonary injury risk assessment for short-duration blasts. J Trauma 2008;65(3):604–615; doi: 10.1097/TA.0b013e3181454ab4
41. Courtney M, Courtney A. Working toward exposure thresholds for blast-induced traumatic brain injury: Thoracic and acceleration mechanisms. Neuroimage 2011;54 (Suppl 1):S55–S61.
42. Simpson EM, Linder CC, Sargent EE, et al. Genetic variation among 129 substrains and its importance for targeted mutagenesis in mice. Nat Genet 1997;16(1):19–27; doi: 10.1038/ng0597-19
43. Ideraabdullah FY, de la Casa-Esperón E, Bell TA, et al. Genetic and haplotype diversity among wild-derived mouse inbred strains. Genome Res 2004;14(10A):1880–1887; doi: 10.1101/gr.2519704
44. Baker CN, Duso D, Kothapalli N, et al. Characterization of collaborative cross mouse founder strain CAST/EiJ as a novel model for lethal COVID-19. Sci Rep 2024;14(1):25147; doi: 10.1038/s41598-024-77087-1
45. Green R, Wilkins C, Thomas S, et al. Oas1b-dependent immune transcriptional profiles of West Nile virus infection in the collaborative cross. G3 (Bethesda) 2017;7(6):1665–1682; doi: 10.1534/g3.117.041624
46. Morgan CN, Matheny AM, Nakazawa YJ, et al. Laboratory infection of novel Akhmeta virus in CAST/EiJ mice. Viruses 2020;12(12):1416; doi: 10.3390/v12121416
47. Nam H, Kim B, Gautam A, et al. Elucidating the characteristics of Mx1 and resistance to influenza a virus subtype H1N1 in the newly developed KWM/Hym mice. Lab Anim Res 2022;38(1):28; doi: 10.1186/s42826-022-00138-z
48. Gullotti DM, Beamer M, Panzer MB, et al. Significant head accelerations can influence immediate neurological impairments in a murine model of blast-induced traumatic brain injury. J Biomech Eng 2014;136(9): 091004; doi: 10.1115/1.4027873 24950710
49. Goldstein LE, Fisher AM, Tagge CA, et al. Chronic traumatic encephalopathy in blast-exposed military veterans and a blast neurotrauma mouse model. Sci Transl Med 2012;4(134):134ra60; doi: 10.1126/scitranslmed.3003716
50. Dal Cengio Leonardi A, Keane NJ, Bir CA, et al. Head orientation affects the intracranial pressure response resulting from shock wave loading in the rat. J Biomech 2012;45(15):2595–2602; doi: 10.1016/j.jbiomech.2012.08.024
51. Dal Cengio Leonardi A, Keane NJ, Hay K, et al. Methodology and evaluation of intracranial pressure response in rats exposed to complex shock waves. Ann Biomed Eng 2013;41(12):2488–2500; doi: 10.1007/s10439-013-0850-2
52. Abràmoff MD. Image processing with ImageJ. Biophotonics Int 2004; 11(7):36–42.
53. The Jackson Laboratory. Jax Frontend Platform. n.d. Available from: https://jax.org [Last accessed: February 19, 2025].
54. Teng MZ, Merenick D, Jessel A, et al. Consistency in reporting of loss of righting reflex for assessment of general anesthesia in rats and mice: A systematic review. Comp Med 2024;74(1):12–18; doi: 10.30802/AALAS-CM-23-000063
55. Balaban C, Jackson RL, Liu J, et al. Intracranial venous injury, thrombosis and repair as hallmarks of mild blast traumatic brain injury in rats: Lessons from histological and immunohistochemical studies of decalcified sectioned heads and correlative microarray analysis. J Neurosci Methods 2016;272:56–68; doi: 10.1016/j.jneumeth.2016.02.001
56. Hayman E, Keledjian K, Stokum JA, et al. Selective vulnerability of the foramen magnum in a rat blast traumatic brain injury model. J Neurotrauma 2018;35(17):2136–2142; doi: 10.1089/neu.2017.5435
57. Jean A, Nyein MK, Zheng JQ, et al. An animal-to-human scaling law for blast-induced traumatic brain injury risk assessment. Proc Natl Acad Sci U S A 2014;111(43):15310–15315; doi: 10.1073/pnas.1415743111
58. Ramsey R, Higbee M, Maesner J, et al. Influence of age on the pharmacokinetics of butorphanol. Acute Care 1988;12 (Suppl 1):8–16.
59. Rifkin JA, Wu T, Rayfield AC, et al. Brain architecture-based vulnerability to traumatic injury. Front Bioeng Biotechnol 2022;10:936082; doi: 10.3389/fbioe.2022.936082
60. Wu T, Rifkin JA, Rayfield AC, et al. Concussion prone scenarios: A multidimensional exploration in impact directions, brain morphology, and network architectures using computational models. Ann Biomed Eng 2022;50(11):1423–1436; doi: 10.1007/s10439-022-03085-x
61. Bass CR, Panzer MB, Rafaels KA, et al. Brain injuries from blast. Ann Biomed Eng 2012;40(1):185–202; doi: 10.1007/s10439-011-0424-0
62. de Lanerolle NC, Bandak F, Kang D, et al. Characteristics of an explosive blast-induced brain injury in an experimental model. J Neuropathol Exp Neurol 2011;70(11):1046–1057; doi: 10.1097/NEN.0b013e318235bef2
63. Percival CJ, Devine J, Hassan CR, et al. The genetic basis of neurocranial size and shape across varied lab mouse populations. J Anat 2022;241(2): 211–229; doi: 10.1111/joa.13657
64. Dobrinskikh E, Estrella AM, Hennessy CE, et al. Genes, other than Muc5b, play a role in bleomycin-induced lung fibrosis. Am J Physiol Lung Cell Mol Physiol 2021;321(2):L440–L450; doi: 10.1152/ajplung.00615.2020
65. Wang KKW, Yang Z, Yue JK, et al. Plasma anti-glial fibrillary acidic protein autoantibody levels during the acute and chronic phases of traumatic brain injury: A transforming research and clinical knowledge in traumatic brain injury pilot study. J Neurotrauma 2016;33(13): 1270–1277; doi: 10.1089/neu.2015.3881
66. Zhang Z, Zoltewicz JS, Mondello S, et al. Human traumatic brain injury induces autoantibody response against glial fibrillary acidic protein and its breakdown products. PLoS One 2014;9(3):e92698; doi: 10.1371/journal.pone.0092698
67. Marchi N, Bazarian JJ, Puvenna V, et al. Consequences of repeated blood-brain barrier disruption in football players. PLoS One 2013;8(3): e56805; doi: 10.1371/journal.pone.0056805
68. Needham EJ, Stoevesandt O, Thelin EP, et al. Complex autoantibody responses occur following moderate to severe traumatic brain injury. J Immunol 2021;207(1):90–100; doi: 10.4049/jimmunol.2001309
69. Raad M, Nohra E, Chams N, et al. Autoantibodies in traumatic brain injury and central nervous system trauma. Neuroscience 2014;281: 16–23; doi: 10.1016/j.neuroscience.2014.08.045
70. Daglas M, Draxler DF, Ho H, et al. Activated CD8+ T cells cause long-term neurological impairment after traumatic brain injury in mice. Cell Rep 2019;29(5):1178–1191.e6; doi: 10.1016/j.celrep.2019.09.046
71. Hernandez A, Tan C, Plattner F, et al. Exposure to mild blast forces induces neuropathological effects, neurophysiological deficits and biochemical changes. Mol Brain 2018;11(1):64; doi: 10.1186/s13041-018-0408-1
72. Heyburn L, Batuure A, Wilder D, et al. Neuroinflammation profiling of brain cytokines following repeated blast exposure. Int J Mol Sci 2023; 24(16):12564; doi: 10.3390/ijms241612564
73. Shetty AK, Mishra V, Kodali M, et al. Blood brain barrier dysfunction and delayed neurological deficits in mild traumatic brain injury induced by blast shock waves. Front Cell Neurosci 2014;8:404; doi: 10.3389/fncel.2014.00232
74. Siva Sai Sujith Sajja B, Tenn C, McLaws LJ, et al. IL-5; a diffuse biomarker associated with brain inflammation after blast exposure. Biomed Sci Instrum 2014;50:375–382.
75. Izzy S, Chen PM, Tahir Z, et al. Association of traumatic brain injury with the risk of developing chronic cardiovascular, endocrine, neurological, and psychiatric disorders. JAMA Netw Open 2022;5(4):e229478; doi: 10.1001/jamanetworkopen.2022.9478
76. Albrecht JS, Kirk J, Ryan KA, et al. Neighborhood deprivation and recovery following traumatic brain injury among older adults. J Head Trauma Rehabil 2025 Mar-Apr 01;40(2):57–64; doi: 10.1097/HTR.0000000000001007
77. Lu K, Liang C-L, Li P-C, et al. Risk factors for myocardial dysfunction after traumatic brain injury: A one-year follow-up study. Injury 2017;48(8): 1794–1800; doi: 10.1016/j.injury.2017.07.004
78. Zimering MB, Patel D, Bahn G. Type 2 diabetes predicts increased risk of neurodegenerative complications in veterans suffering traumatic brain injury. J Endocrinol Diabetes 2019;6(3):137; doi: 10.15226/2374-6890/6/3/001137
79. Haskell BD, Flurkey K, Duffy TM, et al. The diabetes-prone NZO/HlLt strain. I. Immunophenotypic comparison to the related NZB/BlNJ and NZW/LacJ strains. Lab Invest 2002;82(7):833–842; doi: 10.1097/01.lab.0000018915.53257.00

80. Ortlepp JR, Kluge R, Giesen K, et al. A metabolic syndrome of hypertension, hyperinsulinaemia and hypercholesterolaemia in the New Zealand obese mouse. Eur J Clin Invest 2000;30(3):195–202; doi: 10.1046/j.1365-2362.2000.00611.x
81. Faber JE, Zhang H, Xenakis JG, et al. Large differences in collateral blood vessel abundance among individuals arise from multiple genetic variants. J Cereb Blood Flow Metab 2023;43(11):1983–2004; doi: 10.1177/0271678X231194956
82. Friedman MA, Buettmann EG, Zeineddine Y, et al. Genetic variation influences the skeletal response to hindlimb unloading in the eight founder strains of the diversity outbred mouse population. J Orthop Res 2024;42(1):134–140; doi: 10.1002/jor.25646
83. Cekanaviciute E, Tran D, Nguyen H, et al. Mouse genomic associations with *in vitro* sensitivity to simulated space radiation. Life Sci Space Res (Amst) 2023;36:47–58; doi: 10.1016/j.lssr.2022.07.006
84. Taylor MK, Hernández LM, Stump J, et al. Blast exposure interacts with genetic variant 5HTTLPR to predict posttraumatic stress symptoms in military explosives personnel. Psychiatry Res 2019;280:112519; doi: 10.1016/j.psychres.2019.112519

Cite this article as: Georges AP, Browne KD, Augustin DV, et al. Genetic diversity influences response and outcome to blast traumatic brain injury in a murine model, *Neurotrauma Reports* 2026:7(1): 36–53, doi: 10.1177/2689288X251411057.

Abbreviations Used

AMPK = activated protein kinase
AMP = adenosine monophosphate
ANOVA = analysis of variance
BBB = blood-brain barrier
bTBI = blast-induced traumatic brain injury
CC-RIX = Collaborative Cross F1
CC = Collaborative Cross
CI = confidence interval
DO = Diversity Outbred
GFAP = glial fibrillary acidic protein
HR = hazard ratio
IACUC = Institutional Animal Care and Use Committee
ICH = intracranial hemorrhage
IPH = intraparenchymal hemorrhage
IP = intraperitoneally
IVH = intraventricular hemorrhage
J:DO = Jackson Diversity Outbred
LD50 = lethal dose 50
LSD = least significant difference
MAG = myelin-associated glycoprotein
MPP = multiparental population
NK = natural killer
PBS = phosphate buffered saline
PET = polyethylene terephthalate
PHS = Public Health Service
SAH = subarachnoid hemorrhage
SNP = single-nucleotide polymorphism
TBI = traumatic brain injury
T1DM = type 1 diabetes mellitus
T2DM = type 2 diabetes mellitus
w/o = weeks old

Publish in Neurotrauma Reports

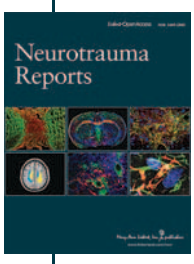

- Immediate, unrestricted online access
- Rigorous peer review
- Compliance with open access mandates
- Authors retain copyright
- Highly indexed
- Targeted email marketing

liebertpub.com/neur